Articles

Measurement of the Phase Behavior of the Ternary System Carbon Dioxide + Acetone + Phenanthrene

Juan C. de la Fuente,[†] Susana B. Bottini,[‡] and Cor J. Peters*,[§]

Departamento de Procesos Químicos, Universidad Técnica Federico Santa María, Casilla de Correo 110-V, Valparaíso, Chile, PLAPIQUI (Universidad Nacional del Sur−CONICET), CC 717-8000 Bahía Blanca, Argentina, and Faculty of Applied Sciences (DelftChemTech), Physical Chemistry and Molecular Thermodynamics, Delft University of Technology, Julianalaan 136, 2628 BL Delft, The Netherlands

As a representative model system for the gas-anti-solvent (GAS) process, the phase behavior of the ternary system carbon dioxide + acetone + phenanthrene has been studied experimentally. Carbon dioxide was chosen as the gaseous anti-solvent, acetone was chosen as the organic solvent, and phenanthrene was chosen as the model solute. In each experiment, a solution of phenanthrene in acetone was expanded using carbon dioxide as the anti-solvent. A synthetic method was used for the measurements of the various phase boundaries. Three-phase equilibrium data solid (phenanthrene)−liquid−vapor were obtained from intersection of two-phase isopleths vapor−liquid and solid−liquid. For a variety of compositions, results are reported for this ternary system within temperature and pressure ranges of (295 to 350) K and (1.0 to 12.5) MPa, respectively. As was established in a previous study on the system carbon dioxide + 2-propanol + salicylic acid, it turned out that also in the system carbon dioxide + acetone + phenanthrene the carbon dioxide concentration significantly affects the optimum operational conditions of the GAS process (i.e., at lower concentrations carbon dioxide acts as a co-solvent, while at higher concentrations it acts as an anti-solvent). Also, it is shown that at a certain temperature, it is possible to precipitate most of the dissolved solute within only a small pressure window.

Introduction

The size and the size distribution of particles produced in the pharmaceutical industry are usually not appropriate for drug delivery in the body. Especially when dealing with aerosol delivery of drugs in the lungs or controlled release of micropowders in the body, a narrow size distribution of fine particles is necessary. So, certain pharmaceutical products need to be micronized in order to do the following: (a) Allow the use of more suitable drug delivery routes in the body. For example, inhalers can be used for treating asthma instead of tablets or injections, which has the advantage that the primary dosage bypasses the liver. (b) Decrease the required dosage of drug, since the efficiency of micronized drugs is higher. (c) Increase the bioavailability of drug in the body. When the controlled release method is used for drug delivery, there is always a rather constant amount of drug in the body. However, when tablets or capsules are used, at the beginning there is a drug peak in the body, diminishing to almost no presence of the drug at the end of the period of dosing.

When a pharmaceutical is micronized, it should retain its original crystallinity and chemical activity. It should also be non-aggregated and free-flowing. Several methods currently are in use for micronizing pharmaceuticals: jet and ball milling, spray drying, and recrystallization using solvent evaporation or liquid anti-solvent. But all these techniques have the disadvan-

tage in common of poor control on the size distribution of the micronized particles (i.e., usually a wide range of particle sizes is produced). In addition, each method has its own specific disadvantages. For example, spray drying usually has high operating temperatures, which may cause thermal degradation of the pharmaceuticals. Solvent evaporation and liquid anti-solvent recrystallization are facing solvent and anti-solvent residual problems. To solve these shortcomings, a number of researchers[1−7] tried to apply new techniques using supercritical fluids that had already been used for micronizing other materials such as explosives, polymers, superconductor precursors, and coloring materials. For a detailed overview of possible techniques, see, for example, refs 8 and 9.

Unfortunately, there is a serious lack of published experimental data on the phase behavior of such systems. Therefore, in this work the phase behavior of the ternary model system carbon dioxide + acetone + phenanthrene has been studied, where phenanthrene has been considered as a model pharmaceutical. Carbon dioxide has been chosen as the anti-solvent gas due to its numerous advantages to apply in the pharmaceutical industry: it is nontoxic nonflammable, and cheap; its critical temperature and pressure are relatively low; its solubility in organic solvents is appreciable; and it has good transport properties.

In this study. vapor−liquid and solid−liquid boundaries of two- and three-phase equilibria have been measured at a variety of conditions in terms of composition, pressure, and temperature. Intersection of corresponding two-phase boundaries vapor−liquid and solid−liquid gave additional information on the three-phase equilibrium solid−liquid-vapor.

* Corresponding author. Phone: +31-15-2782660. Fax: +31-15-2788047. E-mail: Cor.Peters@tnw.tudelft.nl.
† Universidad Técnica Federico Santa María.
‡ PLAPIQUI (Universidad Nacional del Sur−CONICET).
§ Delft University of Technology.

Table 1. Experimentally Determined Vapor−Liquid Boundaries in the Ternary System Carbon Dioxide + Acetone + Phenanthrene ($X_{PH-CO_2 Free}$ = 0.021)

		LV → V			
X_{CO_2}	X_{PH}	T/K	P/MPa	T/K	P/MPa
0.3643	0.0136	295.26	1.956	308.22	2.471
		305.21	2.346	318.17	2.906
		325.04	3.241	328.10	3.386
		315.19	2.781	298.35	2.072
		334.90	3.731	337.94	3.891
		288.58	1.716	342.75	4.146

Table 2. Various Experimentally Determined Phase Transitions in the Ternary System Carbon Dioxide + Acetone + Phenanthrene ($X_{PH-CO_2 Free}$ = 0.198)

		LV → V		SL → L		SLV → LV		SLV → SL	
X_{CO_2}	X_{PH}	T/K	P/MPa	T/K	P/MPa	T/K	P/MPa	T/K	P/MPa
0.3008	0.1383	313.52	2.785	313.58	7.452	309.27	1.602	310.61	2.637
		316.20	2.910	313.20	5.452	310.50	1.955	311.66	2.692
		318.22	3.001	312.88	2.752	311.55	2.212	312.65	2.747
		320.38	3.100			312.29	2.452	312.88	2.752
		322.91	3.226			312.88	2.752		
		324.99	3.320						
		327.95	3.466						
		330.87	3.716						

Table 3. Various Experimentally Determined Phase Transitions in the Ternary System Carbon Dioxide + Acetone + Phenanthrene ($X_{PH-CO_2 Free}$ = 0.302)

		LV → V		SL → L		SLV → LV		SLV → SL	
X_{CO_2}	X_{PH}	T/K	P/MPa	T/K	P/MPa	T/K	P/MPa	T/K	P/MPa
0.3033	0.2103	321.81	3.621	321.81	3.621	319.13	2.805	319.12	3.446
		323.05	3.665	321.79	5.450	320.08	3.117	320.08	3.507
		327.94	3.960	322.02	7.450	321.13	3.421	321.12	3.556
		332.92	4.245			321.81	3.621	321.81	3.621
		337.86	4.535						
		342.81	4.835						
		347.74	5.140						

Table 4. Various Experimentally Determined Phase Transitions in the Ternary System Carbon Dioxide + Acetone + Phenanthrene ($X_{PH-CO_2 Free}$ = 0.099)

		LV → V		SL → L		SLV → LV		SLV → SL	
X_{CO_2}	X_{PH}	T/K	P/MPa	T/K	P/MPa	T/K	P/MPa	T/K	P/MPa
0.3043	0.0691	298.79	1.942	298.83	7.452	295.37	1.315	295.36	1.811
		303.28	2.102	298.71	5.452	296.36	1.552	296.33	1.851
		308.21	2.292	298.79	1.942	297.40	1.677	297.40	1.887
		313.19	2.492			298.09	1.802	298.04	1.917
		318.13	2.697			298.79	1.942	298.79	1.942
		323.07	2.907						
		327.99	3.127						

Table 5. Various Experimentally Determined Phase Transitions in the Ternary System Carbon Dioxide + Acetone + Phenanthrene ($X_{PH-CO_2 Free}$ = 0.050)

		LV → V			
X_{CO_2}	X_{PH}	T/K	P/MPa	T/K	P/MPa
0.2715	0.0363	295.40	1.537	323.09	2.442
		298.33	1.627	328.02	2.587
		303.28	1.777	332.98	2.817
		308.22	1.932	337.91	3.012
		313.17	2.097	342.87	3.217
		318.16	2.267		

Table 6. Various Experimentally Determined Phase Transitions in the Ternary System Carbon Dioxide + Acetone + Phenanthrene ($X_{PH-CO_2 Free}$ = 0.050)

		LV → V		SL → L		SLV → LV		SLV → SL	
X_{CO_2}	X_{PH}	T/K	P/MPa	T/K	P/MPa	T/K	P/MPa	T/K	P/MPa
0.5997	0.0200	300.73	3.851	300.73	3.851	297.39	3.266	297.36	3.596
		313.22	4.801	300.72	5.451	298.36	3.426	298.35	3.671
		318.16	5.226	300.84	7.451	299.39	3.581	299.36	3.746
		323.12	5.641			300.73	3.851	300.73	3.851
		328.08	6.081						
		333.02	6.516						
		337.97	6.976						
		342.93	7.446						

Table 7. Various Experimentally Determined Phase Transitions in the Ternary System Carbon Dioxide + Acetone + Phenanthrene ($X_{PH-CO_2 Free}$ = 0.099)

		LV → V		SL → L		SLV → LV		SLV → SL	
X_{CO_2}	X_{PH}	T/K	P/MPa	T/K	P/MPa	T/K	P/MPa	T/K	P/MPa
0.6007	0.0397	315.04	5.110	315.17	7.450	308.24	3.746	308.24	4.491
		318.13	5.380	315.04	5.450	309.91	4.086	309.92	4.622
		328.00	6.285	315.04	5.110	311.57	4.426	311.56	4.767
		332.94	6.760			313.19	4.736	314.16	5.036
		337.85	7.245			315.04	5.110	315.04	5.110
		342.82	7.745						

Table 8. Various Experimentally Determined Phase Transitions in the Ternary System Carbon Dioxide + Acetone + Phenanthrene ($X_{PH-CO_2 Free}$ = 0.151)

		LV → V		SL → L		SLV → LV		SLV → SL	
X_{CO_2}	X_{PH}	T/K	P/MPa	T/K	P/MPa	T/K	P/MPa	T/K	P/MPa
0.6004	0.0603	326.70	6.792	326.70	6.792	323.17	5.952	323.10	6.337
		329.84	7.132	326.70	8.452	324.18	6.191	323.94	6.441
		332.90	7.476			324.73	6.326	324.94	6.566
		337.80	8.026			325.99	6.621	326.11	6.721
		342.78	8.601			326.70	6.792	326.70	6.792

Experimental Section

Apparatus and Procedures. Experiments were carried out in a Cailletet apparatus according to the synthetic method. In this apparatus, the pressure or temperature can be varied at fixed temperature or pressure, respectively, for a sample with a constant overall composition until a phase change is visually observed. Pressures up to 15 MPa can be applied, and the temperature can range from 250 K up to 450 K.

Essentially, this apparatus is a thick-walled Pyrex glass tube. This Cailletet tube is about 50 cm long and has inner and outer diameters of 3 mm and 10 mm, respectively. A sample of fixed and known overall composition is dosed into the tube. The open end of the tube is placed in an autoclave and immersed in mercury. The mercury serves as a pressure intermediate between the sample and the hydraulic oil of the pressure generating system. It also confines the sample in the Cailletet tube. A stainless steel ball driven by reciprocating magnets stirs the sample. Pressure is generated by means of a screw-type hand pump. A dead weight pressure gauge is used to measure the

pressure inside the autoclave. The accuracy of the pressure measurement is within 0.03 % of the reading. To keep the sample at the desired temperature, a thermostat liquid circulates through a glass jacket surrounding the glass tube. The thermostat bath is capable of maintaining the thermostat liquid at the desired temperature with a constancy better than ± 0.01 K. A platinum resistance thermometer records the temperature near the vicinity of the sample. The maximum error of this thermometer is about ± 0.02 K. Further details of the apparatus, the experimental procedures, and the reproducibility of measurements of the Cailletet facility type can be found elsewhere.[10,11]

Chemicals. Phenanthrene (purity > 99.5 mol %) and acetone (purity > 99 mol %) were obtained from J. K. Baker, and carbon dioxide (purity 99.995 mol %) was from Hoek-Loos. All chemicals were used without any further purification.

Results and Discussion

Tables 1 to 10 summarize the primary experimental data of the various types of phase transition data (i.e., vapor−liquid, solid−liquid, liquid−liquid, solid−liquid−vapor, and liquid−
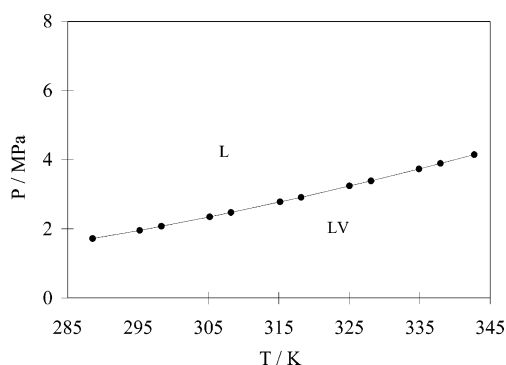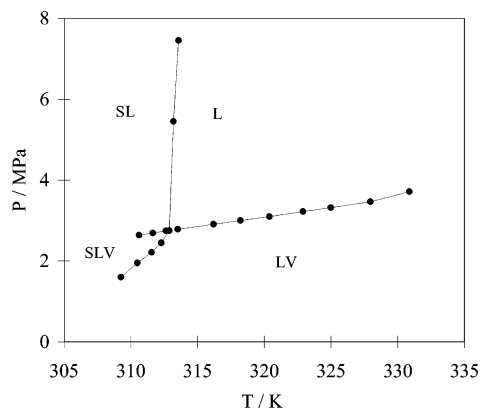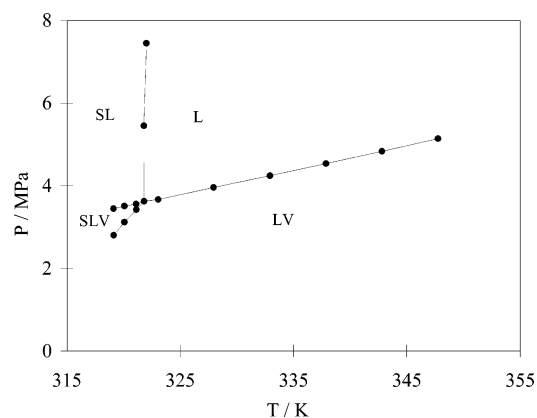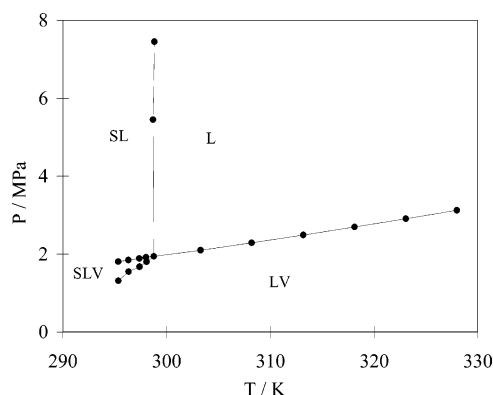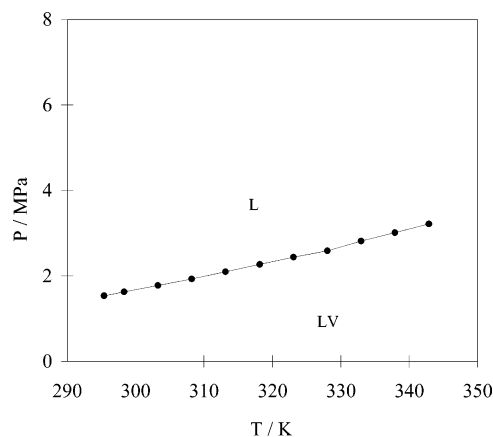
Table 9. Various Experimentally Determined Phase Transitions in the Ternary System Carbon Dioxide + Acetone + Phenanthrene ($X_{PH-CO_2\ Free} = 0.050$)

		LLV → LL		SL → LL		SLV → LV		SLV → SL	
X_{CO_2}	X_{PH}	T/K	P/MPa	T/K	P/MPa	T/K	P/MPa	T/K	P/MPa
0.9001	0.0050	338.54	10.353	338.54	10.353	332.90	9.027	298.34	5.597
		339.85	10.456	338.54	11.953	334.99	9.263	303.27	6.182
		342.84	10.687			338.54	9.653	308.22	6.782
		347.76	10.986					313.17	7.417
								318.13	8.077
		LLV → LV						323.15	8.702
		338.54	9.652					328.01	9.307
		339.80	9.826					332.90	9.822
		342.85	10.122					335.01	10.026
		347.77	10.381					337.54	10.261

Table 10. Various Experimentally Determined Phase Transitions in the Ternary System Carbon Dioxide + Acetone + Phenanthrene ($X_{PH-CO_2\ Free} = 0.050$)

		LV → V		SL → L		SLV → LV		SLV → SL	
X_{CO_2}	X_{PH}	T/K	P/MPa	T/K	P/MPa	T/K	P/MPa	T/K	P/MPa
0.7504	0.0124	316.61	6.572	316.62	7.452	303.32	4.112	298.40	4.702
		323.15	7.312	316.62	8.203	308.31	5.037	303.30	5.162
		328.06	7.882	316.61	6.572	313.26	5.952	308.27	5.672
		333.07	8.472			316.61	6.572	313.24	6.207
		337.93	9.072					316.61	6.572
		342.93	9.667						

liquid−vapor). Each table represents a fixed overall composition of the ternary system. In addition, for each fixed overall composition Figures 1 to 10 give a graphical representation of the experimentally determined phase behavior. As can be seen from these figures, seven of them (Figures 2 to 4, 6 to 8, and 10) have the same qualitative shape: intersection of the two-

Figure 1. Experimentally determined vapor−liquid boundaries in the ternary system carbon dioxide + acetone + phenanthrene ($X_{PH-CO_2\ Free} = 0.021$). Dots are experimental data (Table 1), and the full curves are best fits to the data.

Figure 2. Various experimentally determined phase transitions in the ternary system carbon dioxide + acetone + phenanthrene ($X_{PH-CO_2\ Free} = 0.198$). Dots are experimental data (Table 2), and the full curves are best fits to the data.

Figure 3. Various experimentally determined phase transitions in the ternary system carbon dioxide + acetone + phenanthrene ($X_{PH-CO_2\ Free} = 0.302$). Dots are experimental data (Table 3), and the full curves are best fits to the data.

Figure 4. Various experimentally determined phase transitions in the ternary system carbon dioxide + acetone + phenanthrene ($X_{PH-CO_2\ Free} = 0.099$). Dots are experimental data (Table 4), and the full curves are best fits to the data.

Figure 5. Experimentally determined vapor−liquid boundaries in the ternary system carbon dioxide + acetone + phenanthrene ($X_{PH-CO_2\ Free} = 0.050$). Dots are experimental data (Table 5), and the full curves are best fits to the data.

phase boundaries vapor−liquid at the three-phase locus solid−liquid−vapor. It is clearly demonstrated that the three-phase equilibrium comprises a region. Although both Figures 1 and 5 will have a similar shape as the ones discussed previously, the phenanthrene concentration is so low that the solid−liquid two-phase boundary is located at much lower temperatures, and so is the three-phase region solid−liquid−vapor. Figure 9 represents an overall composition with on one hand a low phenanthrene concentration and on the other hand a high CO_2
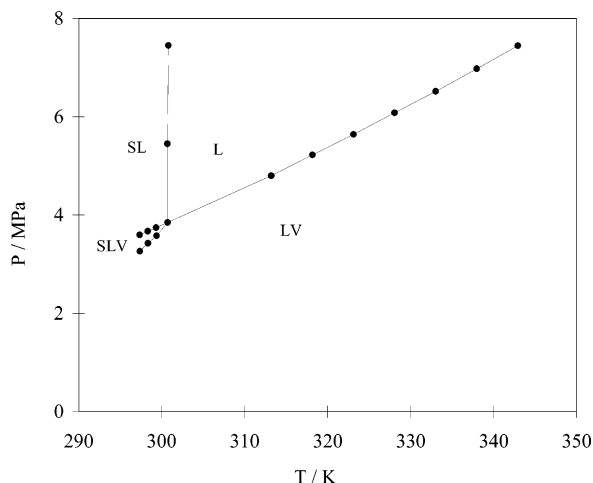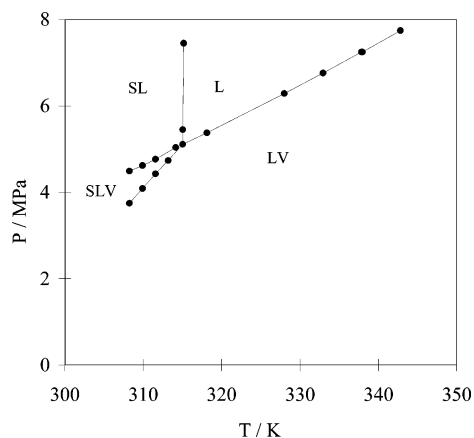
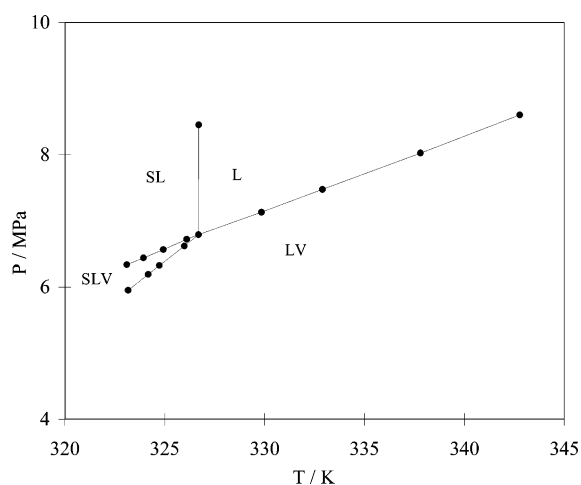**Figure 6.** Various experimentally determined phase transitions in the ternary system carbon dioxide + acetone + phenanthrene ($X_{PH-CO_2\ Free} = 0.050$). Dots are experimental data (Table 6), and the full curves are best fits to the data.

Figure 7. Various experimentally determined phase transitions in the ternary system carbon dioxide + acetone + phenanthrene ($X_{PH-CO_2\ Free} = 0.099$). Dots are experimental data (Table 7), and the full curves are best fits to the data.

Figure 8. Various experimentally determined phase transitions in the ternary system carbon dioxide + acetone + phenanthrene ($X_{PH-CO_2\ Free} = 0.151$). Dots are experimental data (Table 8), and the full curves are best fits to the data.

concentration. These are typically the conditions at which liquid−liquid immiscibility is likely to occur, which indeed turned out to be the case.
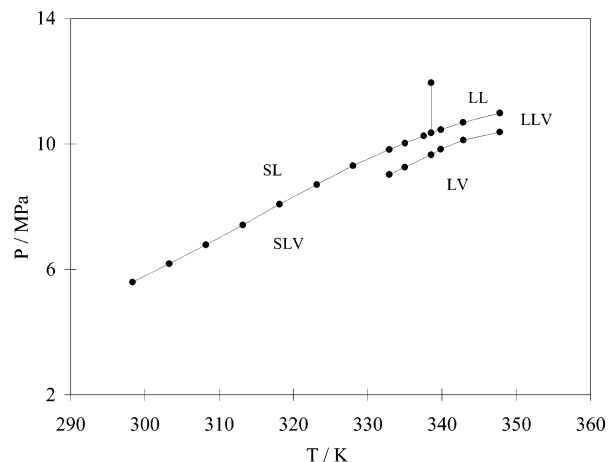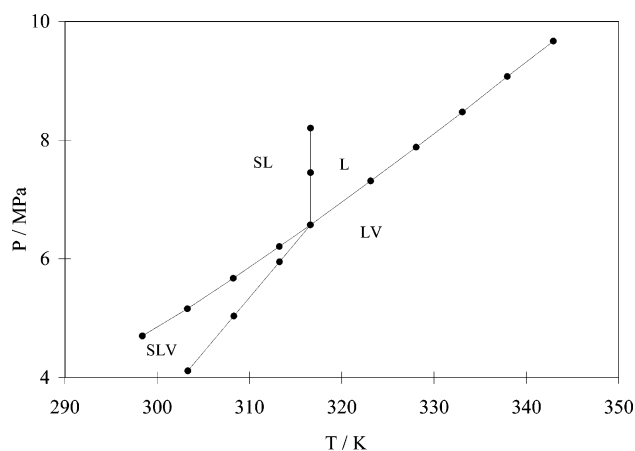

Figure 9. Various experimentally determined phase transitions in the ternary system carbon dioxide + acetone + phenanthrene ($X_{PH-CO_2\ Free} = 0.050$). Dots are experimental data (Table 9), and the full curves are best fits to the data.

Figure 10. Various experimentally determined phase transitions in the ternary system carbon dioxide + acetone + phenanthrene ($X_{PH-CO_2\ Free} = 0.050$). Dots are experimental data (Table 10), and the full curves are best fits to the data.
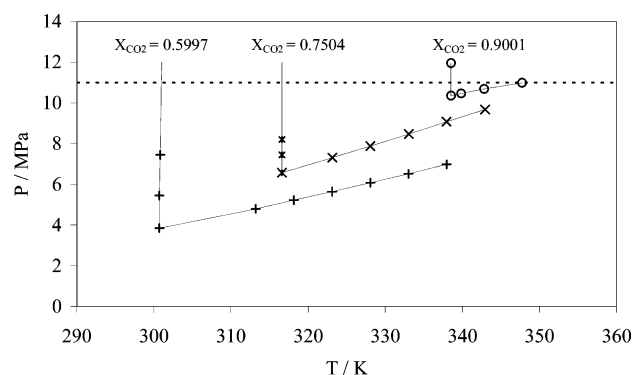

Figure 11. Intersection of corresponding vapor−liquid and solid−liquid isopleths for a molar fraction of phenanthrene (CO₂-free basis). Data taken from Tables 6, 9, and 10. The dashed line determines the solubility of solid phenanthrene as a function of the CO₂ mole fraction at a fixed pressure of 11 MPa.

Figure 11 shows the vapor−liquid and solid−liquid two-phase boundaries, including their point of intersection, which is a point of the three-phase locus solid−liquid−vapor. All data present in this figure have a phenanthrene mole fraction of 0.05 on a CO₂-free basis but at different CO₂ mole fractions (see Figure 11). At a pressure of 11 MPa, the points of interection are determined with the three solid−liquid two-phase boundaries.
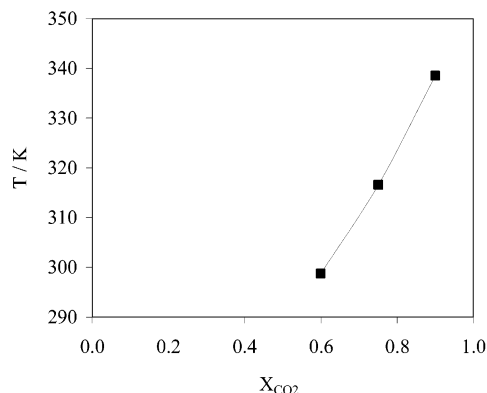
Figure 12. Solubility of solid phenanthrene as a function of temperature and CO_2 mole fraction at a fixed pressure of 11 MPa (see Table 11).

Table 11. Precipitation Temperature vs X_{CO_2} at 11 MPa ($X_{PH-CO_2\ Free} = 0.050$)

X_{CO_2}	T/K
0.5997	298.75
0.7504	316.60
0.9001	338.50

Table 11 gives the numerical values of the points of intersection, and in Figure 12 these points of intersection are shown graphically as a function of temperature versus the CO_2 mole fraction. From Figure 12, it becomes apparent that with increasing CO_2 mole fraction the temperature at which solid phenan-threne starts to precipitate increases (i.e., CO_2 is acting as an anti-solvent in the mixture). This is in agreement with previous observations, for instance in the system CO_2 + 1-propanol + salicylic acid.[12]

Conclusions

To have insight in the optimum design of the GAS process for the recrystallization of pharmaceuticals, phase behavior data on ternary model systems are important. This study offers a new system to the scarce collection of available systems (i.e., the system carbon dioxide + acetone + phenenthrene). As was already found in a previous study,[13] the CO_2 concentration greatly affects the phase behavior of the system. At relatively high concentrations, CO_2 starts to act as an anti-solvent. At very high concentrations, CO_2 forces the system to show liquid−liquid immiscibility.

Literature Cited

(1) Reverchon, E.; Della Porta, G.; Falivene, M. G. Process parameters and morphology in amoxicillin micro and submicro particles generation by supercritical antisolvent precipitation, *J. Supercrit. Fluids* **2000**, *17*, 239.

(2) Thiering, R.; Dehghani, F.; Dillow, A.; Foster, N. R. The influence of operating conditions on the dense gas precipitation of model proteins. *J. Chem. Technol. Biotechnol.* **2000**, *75*, 29.

(3) Reverchon, E.; Della Porta, G. Production of antibiotic micro- and nano-particles by supercritical antisolvent precipitation. *Powder Technol.* **1999**, *106*, 23.

(4) Jaarmo, S.; Rantakyla, M.; Aaltonen, O. Particle tailoring with supercritical fluids: production of amorphous pharmaceutical particles. In *Proceedings of the Fourth International Symposium on Supercritical Fluids*; Arai, K., Ed.; 1997; p 263.

(5) Hanna, M.; York, P.; Shekunov, B. Y., Control of the polymorphic forms of a drug substance by solution enhanced dispersion by supercritical fluids (SEDS). In *Proceedings of the Fourth International Symposium on Supercritical Fluids*; Arai, K., Ed.; 1997; p 325.

(6) Winters, M. A.; Knutson, B. L.; Debenedetti, P. G.; Sparks, H. G.; Przybycien, T. M.; Stevenson, C. L.; Prestrelski, S. J. Precipitation of proteins in supercritical carbon dioxide. *J. Pharm. Sci.* **1996**, *85*, 586.

(7) Yeo, S. D.; Lim, G. B.; Debenedetti, P. G.; Bernstein, H. Formation of microparticulate protein powders using a supercritical fluid anti-solvent, *Biotechnol. Bioeng.* **1993**, *41*, 341.

(8) Tavana, A.; Randolph, A. D. Isobaric−isothermal fractional crystallization of organic solids from supercritical fluid mixtures. *AIChE Symp. Ser.* **1991**, *No. 284*, 5.

(9) Shariati, A.; Peters, C. J. Recent developments in particle design using supercritical fluids. *Solid State Mater. Sci.* **2004**, *7/4−5*, 371.

(10) Chang, C. J.; Randolph, A. D. Solvent expansion and solute solubility predictions in gas-expanded liquids. *AIChE J.* **1990**, *36*, 939.

(11) Peters, C. J.; de Roo, J. L. Measurements and calculations of phase equilibria of binary mixtures of ethane + eicosane. Part I: vapor + liquid equilibria. *Fluid Phase Equilib.* **1987**, *34*, 287.

(12) Peters, C. J.; de Roo, J. L.; Swaan Arons, J. Phase equilibria in binary mixtures of propane and hexacontane. *Fluid Phase Equilib.* **1993**, *85*, 301.

(13) Shariati, A.; Peters, C. J. Measurements and modeling of the phase behavior of ternary systems of interest for the GAS process: I. The system carbon dioxide + 1-propanol + salicylic acid. *J. Supercrit. Fluids* **2002**, *23*, 195.